EBioMedicine 11 (2016) 73–84

Contents lists available at ScienceDirect

EBioMedicine

journal homepage: www.ebiomedicine.com

Research Paper

Determinants of host susceptibility to murine respiratory syncytial virus (RSV) disease identify a role for the innate immunity scavenger receptor MARCO gene in human infants

Monica High [a,1], Hye-Youn Cho [a,1], Jacqui Marzec [a,1], Tim Wiltshire [b], Kirsten C. Verhein [a], Mauricio T. Caballero [c], Patricio L. Acosta [c,d], Jonathan Ciencewicki [a], Zackary R. McCaw [a], Lester Kobzik [e], Laura Miller-DeGraff [a], Wes Gladwell [a], David B. Peden [f], M. Elina Serra [c], Min Shi [g], Clarice Weinberg [g], Oscar Suzuki [b], Xuting Wang [h], Douglas A. Bell [h], Fernando P. Polack [c,i,*], Steven R. Kleeberger [a,**]

[a] Immunity, Inflammation, and Diseases Laboratory, National Institute of Environmental Health Sciences, Research Triangle Park, NC, USA
[b] Division of Pharmacotherapy and Experimental Therapeutics, Eshelman School of Pharmacy, University of North Carolina, Chapel Hill, NC, USA
[c] Fundación INFANT, Buenos Aires, Argentina
[d] Consejo Nacional de Investigaciones Cientificas y Tecnicas (CONICET), Buenos Aires, Argentina
[e] Department of Environmental Health, Harvard University School of Public Health, Boston, MA, USA
[f] Center for Environmental Medicine, Asthma and Lung Biology, School of Medicine, University of North Carolina at Chapel Hill, Chapel Hill, NC, USA
[g] Biostatistics and Computational Biology Branch, National Institute of Environmental Health Sciences, Research Triangle Park, NC, USA
[h] Genome Integrity & Structural Biology Laboratory, National Institute of Environmental Health Sciences, Research Triangle Park, NC, USA
[i] Department of Pediatrics, Vanderbilt University, Nashville, TN, USA

ARTICLE INFO

Article history:
Received 15 October 2015
Received in revised form 2 August 2016
Accepted 5 August 2016
Available online 6 August 2016

Keywords:
Infectious disease
Innate immunity
Lung
Single nucleotide polymorphism
SNP
Promoter
Haplotype

ABSTRACT

Background: Respiratory syncytial virus (RSV) is the global leading cause of lower respiratory tract infection in infants. Nearly 30% of all infected infants develop severe disease including bronchiolitis, but susceptibility mechanisms remain unclear.
Methods: We infected a panel of 30 inbred strains of mice with RSV and measured changes in lung disease parameters 1 and 5 days post-infection and they were used in genome-wide association (GWA) studies to identify quantitative trait loci (QTL) and susceptibility gene candidates.
Findings: GWA identified QTLs for RSV disease phenotypes, and the innate immunity scavenger receptor *Marco* was a candidate susceptibility gene; targeted deletion of *Marco* worsened murine RSV disease. We characterized a human *MARCO* promoter SNP that caused loss of gene expression, increased in vitro cellular response to RSV infection, and associated with increased risk of disease severity in two independent populations of children infected with RSV.
Interpretation: Translational integration of a genetic animal model and in vitro human studies identified a role for *MARCO* in human RSV disease severity. Because no RSV vaccines are approved for clinical use, genetic studies have implications for diagnosing individuals who are at risk for severe RSV disease, and disease prevention strategies (e.g. RSV antibodies).

1. Introduction

RSV is the primary cause for hospitalization during the first year of life in infants worldwide, and it is the leading cause of lower respiratory tract infection leading to bronchiolitis, pneumonia, and respiratory failure (Lozano et al., 2012). RSV is also a significant cause of respiratory illness in immunocompromised adults and the elderly (Falsey et al., 2005). While the majority of infected subjects present symptoms, the nature and severity of the symptoms vary among individuals (Ciencewicki et al., 2014; Caballero et al., 2015). For some, infection induces cold-like symptoms; others require hospitalization, and a small

* Correspondence to: F.P. Polack, Vanderbilt University, Department of Pediatrics, B-3307 MCN, 1161 21st Ave South, Nashville, TN 37232-2007, USA.
** Corresponding author at: Immunity, Inflammation, and Diseases Laboratory, National Institute of Environmental Health Sciences (NIEHS), 111 T.W. Alexander Drive, Building 101, MD D-201, Research Triangle Park, NC 27709, USA.
E-mail addresses: fernando.p.polack@vanderbilt.edu (F.P. Polack), kleeber1@niehs.nih.gov (S.R. Kleeberger).
[1] These authors contributed equally to this work.

http://dx.doi.org/10.1016/j.ebiom.2016.08.011

percentage of cases require intensive care and may result in death. The wide variation in response to RSV infection suggests that susceptibility and disease are influenced by multiple host intrinsic factors (Stark et al., 2002; Miyairi and DeVincenzo, 2008; Gelfand, 2012; Feldman et al., 2015).

Previous in vivo mouse studies suggest that RSV infectivity is a multigenic trait, but did not identify the genes responsible for infection (Prince et al., 1979; Stark et al., 2002; Stark et al., 2010). The innate and acquired immune systems have been implicated in the pathogenesis of RSV infection, including surfactant association proteins, viral response receptors and proteins, and inflammatory cells and their products such as chemokines, cytokines, and soluble inflammatory mediators [e.g. (Mukherjee and Lukacs, 2013; Varga and Braciale, 2013)]. However, roles for each of these components in the pathogenesis of RSV disease are unclear.

RSV disease is complex and, while candidate gene single nucleotide polymorphisms (SNPs) have associated with RSV disease severity in infants [e.g. (Miyairi and DeVincenzo, 2008; Daley et al., 2012; Ciencewicki et al., 2014; Caballero et al., 2015)], the mechanisms of differential disease susceptibility remain unclear. To better understand the genetic basis of RSV disease, we performed a genome-wide association (GWA) study of disease following infection in inbred strains of mice to identify candidate quantitative trait loci (QTL) and genes that associate with specific disease phenotypes. We identified 7 significant and 8 suggestive QTLs and candidate susceptibility genes including macrophage receptor with collagenous structure (*Marco*), an innate immunity scavenger receptor. Targeted deletion of mouse *Marco* worsened RSV disease phenotypes, consistent with a protective role in disease pathogenesis. We then identified and characterized in vitro a human *MARCO* promoter SNP that diminished mRNA expression basally and after RSV infection. The SNP is located in an antioxidant response element (ARE) of the *MARCO* promoter and is a binding site for the transcription factor nuclear factor (erythroid derived)-2 like 2 (NFE2L2), also known as nuclear factor erythroid 2 (NF-E2)-related factor 2 (NRF2). Deletion of the ARE also reduced *MARCO* mRNA expression following RSV infection in airway epithelial cells. Moreover, compared to the wild-type C allele, we found that the *MARCO* promoter rs1318645 SNP G allele associated with increased disease severity in populations of RSV-infected infants. Our modeling of disease after RSV infection in mice thus identified a host susceptibility gene candidate that has implications for better understanding human disease.

2. Materials and Methods

2.1. Mice and Treatments

Mice from 30 inbred strains (male, 6–10 weeks) for the strain screen were purchased from Jackson Laboratory (Bar Harbor, ME) and housed singly with hardwood bedding (PJ Murphy Forest Products Company, Montville, NJ) in pathogen-free facilities at NIEHS. A breeding colony of *Marco* deficient mice (*Marco*$^{-/-}$) was developed and maintained at NIEHS (Arredouani et al., 2004; Cho et al., 2012). Age- and sex-matched C57BL/6 wild-type (WT) mice were purchased from Charles River Laboratories (Wilmington, MA) and used as controls for experiments with the *Marco*$^{-/-}$ mice. All mice were provided free access to water and pelleted open-formula rodent diet NIH-07 (Zeigler Brothers, Gardners, PA.). Constant air temperature (72 ± 3° F), relative humidity (50 ± 15%), and light/dark cycle (12 h on/12 h off) were maintained during the experiments. Mice of each strain were randomly assigned to either RSV infection or vehicle control groups. Mice were infected in the morning with 10^6 plaque-forming units (PFU) of human RSV-19 strain in 50 μl Hank's balanced salt solution (HBSS) by intranasal instillation, and returned to their cages. HBSS containing HEp-2 cell lysates were intranasally instilled for vehicle controls. On post-instillation days 1 and 5, mice (6–12 per group) were killed by overdose with Nembutal (sodium pentobarbital; 104 mg/kg body weight). Phenotyping for response to RSV infection was performed in at least two separate experiments (n ≥ 3 per group), and power calculations based on previous studies were used to determine sample sizes. All animal use was approved by the NIEHS Animal Care and Use Committee. Animals were treated humanely and with regard to alleviation of suffering.

2.2. Lung Bronchoalveolar Lavage Fluid (BALF) and Cell Preparation

The right lung of each mouse was lavaged in situ consecutively four times with HBSS (35 ml/kg body weight, pH 7.2–7.4) and BALF was analyzed for cell differentials using standard morphological and cytological criteria as described previously (Saltini et al., 1984; Cho et al., 2001). Total protein content (a marker of lung permeability) was measured with the Bradford assay as previously described (Cho et al., 2001; Cho et al., 2007). Investigators were blinded to treatment for all lavage and histopathology samples (see below). Time points chosen for evaluation of inflammation and injury were based on a previous investigation of phenotype kinetics in lungs of a panel of 5 inbred strains of mice infected with RSV (data not shown). We found that the peaks of inflammation and injury phenotypes are time-dependent and usually occur either 1 or 5 days after infection as described previously (Cho et al., 2009).

2.3. Lung Histopathology

Left lung lobes were inflated intratracheally in situ and fixed with 10% neutral buffered zinc formalin for 24 h following procedures described previously (Cho et al., 2009). Fixed lungs were then placed in 70% ethanol until proximal and distal intrapulmonary axial tissues were excised and embedded in paraffin and sectioned (5 μm). Tissue sections were stained histochemically with hematoxylin and eosin (H&E) for histopathological analyses and alcian blue-periodic acid shift (AB/PAS) double staining to identify acidic and neutral mucosubstances (Cho et al., 2009).

2.4. Measurement of Stored Intraepithelial Mucus (Volume Density, VS)

Images of histological sections were captured using an Axioskop 40 microscope, camera, and Axiovision software. Black and white images were taken with a 10× objective lens and analyzed with Scion image analysis software. The mucus-containing area and the perimeter of basal lamina from large airways, visually judged to be third generation bronchus, were used for analysis. The volume of mucus per airway was calculated as described previously (Harkema et al., 1987).

VS values (nl/mm^2 basal lamina) were calculated for each lung section and averaged for vehicle control and RSV infected groups. VS calculations were averaged for each treatment group and are reported as the mean ± SEM for each strain (n = 3/infection/strain).

2.5. Quantitative Real-time Polymerase Chain Reaction (qRT-PCR)

Total RNA was isolated from non-lavaged left lung pieces using RNeasy Mini Kits (Qiagen, Valencia, CA) following manufacturer procedures and as described previously (Cho et al., 2009). Quantification of gene expression was determined by ΔC_T values obtained by subtracting fluorescence detected number of cycles to threshold (C_T) of 18s mRNA from those of target gene RNA in the same sample.

2.6. Heritability and Correlation of Phenotypes

Heritability estimates were calculated following methods described previously (Lightfoot et al., 2004; Nichols et al., 2014). Heritability estimates > 35% were considered sufficient for GWA studies with 30 inbred strains of mice (Tsaih and Korstanje, 2009). Relatedness of RSV disease phenotypes was done using Pearson's correlation coefficients (Gene Network, http://www.genenetwork.org). The maximum

response [1 or 5 days post-infection (PI)] for each phenotype was used for all analyses.

2.7. Genome-wide Association Mapping

GWA mapping was performed using the mean value for each phenotype for each strain. Data for each strain were distributed normally (no outliers removed), and no transformations were applied. We also generated a RSV disease index by performing a principal components (PC) analysis of each quantitated phenotype and then applied the first 3 PCs for each strain to haplotype association mapping. Two different haplotype-based approaches were used: SNPster (Genomics Institute, Novartis Research Foundation, San Diego, CA) and FastMap (University of North Carolina, Chapel Hill, NC). The algorithms (Pletcher et al., 2004; Gatti et al., 2009) and rationale for using these approaches have been described elsewhere (McClurg et al., 2006; Nichols et al., 2014). Experimental informative SNP genotypes for GWA mapping were selected as described previously (Benton et al., 2012). The SNPs used for the 30 strains of mice were fully genotyped (i.e. not imputed). $-\mathrm{Log}_{10}$ P values were considered significant if they exceeded 6.60 (genome-wide significance at $P < 0.05$) and suggestive if they exceeded 6.06 (genome-wide suggestive at $P < 0.20$). Only QTLs that were identified using both algorithms were considered further for candidate gene analyses. Candidate gene SNP and haplotype data were obtained from the Mouse Phenome Database (MPD; Jackson Laboratory; http://phenome.jax.org; dbSNP 138 annotation). Non-informative SNPs (i.e. no heterozygosity between strains or the minor allele was found in <10% of the strains) were removed from further haplotype and SNP analyses. *Marco* haplotype data were obtained from the MPD, and hierarchical clustering was performed as described previously (Cho et al., 2015).

2.8. Sequencing of MARCO Promoter and Functional Assessment

We used traditional walk-down sequencing to identify regions of *MARCO* that were polymorphic, and confirmed these sites by screening an ethnically diverse panel of individuals for allelic variation. Regions with SNPs at 5% or higher frequency were used in promoter deletion experiments to test for effects on transcriptional activity. Constructs were generated to encompass the full length of the *MARCO* promoter (−1388 to +98), and polymorphic regions were sequentially deleted to assess differential activity.

Initial promoter deletion assays identified a polymorphic region of the *MARCO* promoter with high activity (−300 and +98) that contained a putative NRF2-binding ARE. To determine whether the SNP region influenced transcript levels, the −300 to +98 region of *MARCO* containing the rs1318645, −156 C/G SNP (−157) was cloned upstream of the luciferase reporter gene and its expression analyzed by transient transfection using reporter assays. The −300 to −71 promoter region was further investigated by generating two constructs [−300 to +98 bp, (300-Luc) and −71 to +98 bp (71-Luc, lacking the SNP)] and comparing their promoter activity.

To examine effects of the promoter SNP on transcriptional activity, we amplified the 5′-flanking region of genomic *MARCO* promoter to generate polymorphic variants of the 300-Luc sequence [−156 C-Luc and −156 G-Luc]. All constructs were verified by sequencing, and transiently transfected using Fugene HD (Promega, Madison, WI) into BEAS-2B cells (The American Type Culture Collection, Manassas, VA), and analyzed for luciferase activity as described previously (Cho et al., 2015).

For RSV infection we used the pGL4.20 vector, and Beas2B cells were transfected with *MARCO* promoter constructs (−156 C-Luc, −156 G-Luc or −71-Luc) overnight and were serum starved for 1 h during RSV infection (MOI of 4). Cells were harvested 3, 6, 24, 48 and 72 h post-infection. Luciferase activity was assessed in three independent samples and all experiments were repeated in triplicate.

2.9. Electrophoretic Mobility Shift Assay (EMSA)

EMSA allows visualization of transcription factor binding affinity to regulatory promoter sequences in the presence of variant alleles. DNA-protein binding specificity was further assessed using antibodies specific to the binding factor of interest. An aliquot (5 μg) of human lung nuclear protein (Active Motif, Carlsbad, CA) was incubated on ice with binding buffer for 15 min, followed by addition of 3×10^4 cpm [γ^{32}P] ATP (Amersham Biosciences, Piscataway, NJ) end-labeled wild type or variant probes (End-labeled probes: rs1318645 −156 C (wt) FORWARD 5′-CCT GGG AGT GAC GGG TGC ATT CAG AG-3′, REVERSE 5′-CT CTG AAT GCA CCC GTC ACT CCC AGG-3′; rs1318645 −156G (variant) FORWARD 5′-CCT GGG AGT GAG GGG TGC ATT CAG AG-3′, REVERSE 5′-CT CTG AAT GCA CCC CTC ACT CCC AGG-3′) and incubated for 30 min at room temperature. We used short (26 base pairs) fragment sequences for the EMSA experiments that overlap the consensus sequence for *NRF2*. We used polyclonal rabbit anti-NRF2 antiserum (2 μl) or control IgG (2 μl) as controls and processed for EMSA as described previously (Marzec et al., 2007). Samples were electrophoresed and autoradiographed with an intensifying screen at −70 °C. Genotyping was done without knowledge of disease status (i.e. blinded to case or control). We tested for statistically significant differences in DNA-NRF2-antibody complex formation between wild-type, heterozygous, and variant genotypes using one-way ANOVA with SNK a posteriori comparisons of means.

2.10. Human RSV Disease Population

Two independent prospective case-control studies were conducted in Buenos Aires, Argentina from 2003 to 2006 (population 1) and 2010–2013 (population 2); these studies, with inclusion and exclusion criteria, were described previously (Caballero et al., 2015). Study participants were previously healthy full-term infants younger than 1 year of age and born after 15 September of the previous year (i.e. approximately 15 days after the end of RSV season in Buenos Aires). Participants had bronchiolitis symptoms for the first time in their lives, and clinical signs included wheezing with or without cough, rales, dyspnea, and increased respiratory rate and retractions of the respiratory muscles. Diagnosis was performed by trained pediatricians. Infants were tested for RSV, rhinoviruses, hPIV1–4, influenza virus A and B, and human metapneumovirus, and all participating subjects were infected only with RSV. Recruited cases were infants with bronchiolitis whose oxygen saturation upon enrollment was <93% in room air (the primary outcome). Oxygen saturation is a clinically relevant phenotype for discriminating between mild and severe RSV disease (Caballero et al., 2015). Infants with bronchiolitis were recruited as controls if oxygen saturation upon enrollment was ≥93% while breathing room air. Genotyping of infants was performed using whole blood samples (population 1) or nasal aspirates (population 2). Population sizes were based on calculations to provide sufficient statistical power (~80%) to find significant differences between mild and severe disease with a minor allele frequency of ~0.2. The Institutional Review Boards (IRB) of the participating hospitals in Buenos Aires, as well as the Johns Hopkins University IRB (Baltimore, MD, USA), approved the protocol. We obtained informed consent from parents of each infant enrolled in the studies. The study conformed to standards indicated by the Declaration of Helsinki.

2.11. Allelic Discrimination Genotyping for MARCO rs1318645

Genomic DNA was isolated and characterized for purity and concentration as described previously (Caballero et al., 2015). The *MARCO* rs1318645 promoter variant was assessed by allelic discrimination with a predesigned SNP genotyping assay from Applied Biosystems. PCR was performed using 20 μl reactions with 5 ng of genomic DNA, 10 μl of TaqMan 2XPCR Master Mix, and 1.0 μl of 20× pre-optimized

assay mix (C_9566534_20). The 20× mix consisted of 18 μM forward and reverse primers and 8 μM of each allele-specific fluorescently labeled (VIC or FAM) TaqMan MGB probe. Standard PCR cycling conditions were used as described previously (Caballero et al., 2015).

Allele-specific PCR products were detected and verified as described previously (Caballero et al., 2015). Five percent of the samples were repeated for quality control, and we found 100% concordance.

2.12. Statistical Analysis

Lavage and tissue parameters were analyzed by 3-way ANOVA (factors: exposure, time, strain) and Student-Newman-Keuls (SNK) comparisons of means procedures. Strain distribution patterns and *Marco* haplotype groups were analyzed by 1-way ANOVA and SNK comparisons of means. Statistical associations between candidate gene

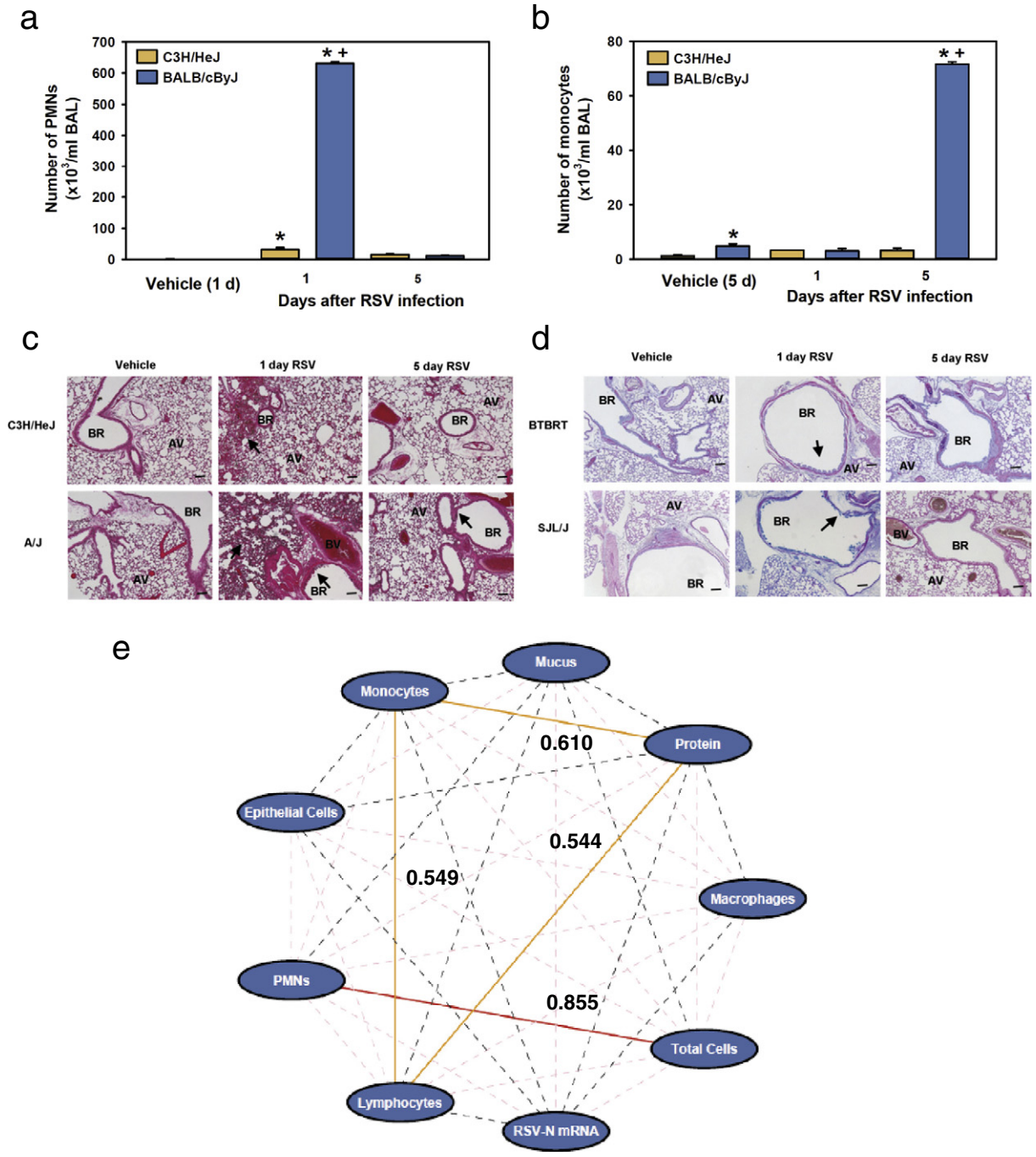

Fig. 1. Lung phenotypes in representative mouse strains with mild and severe disease after infection with RSV. Numbers of PMNs (a) and monocytes (b) found in BALF from C3H/HeJ (mild disease) and BALB/cJ (severe disease) mice following vehicle or RSV infection (1, 5 days PI). Mean ± SEM (n = 6–12 mice/group). Groups were analyzed by 3-way ANOVA and Student-Newman-Keuls a posteriori tests. *P < 0.05 versus vehicle. $^{+}$P < 0.05 versus C3H/HeJ. (c) Representative H&E stained lung sections from C3H/HeJ (mild disease) and A/J (severe disease) mice following vehicle and RSV infection (1, 5 days PI). (d) Representative AB/PAS double stained lung sections from BTBR_T + _tf/J (mild disease) and SJL/J (severe disease) mice following vehicle and RSV infection (1, 5 days PI). Arrows = areas of increased airway inflammation and bronchial epithelial proliferation (hyperplasia). AV = Alveoli, BR = bronchus or bronchiole, BV = blood vessel. Bar = 100 μm. (e) Circular node and edge representation of relatedness between RSV response phenotypes among all mouse strains. Pearson correlation coefficients (R) noted on edges (solid lines) indicate associations between phenotypes. R values ≥ 0.48, P < 0.05; R values ≥ 0.73, P < 0.01.

genotypes and phenotypes within mouse strains were calculated using the two-tailed Student's *t*-test. Only the significance of murine non-synonymous coding SNPs were tested in this study; if more than one non-synonymous coding SNP was found within a gene multiple comparisons were performed. Because of potential bias effects of admixture in our human study populations, we followed methods described previously to test for evidence of bias due to population stratification (Epstein et al., 2007) using 33 ancestral informative markers (AIMs; Suppl. Table S1) that were evaluated in 300 infants with mild or severe RSV disease. Genotyping was performed on the Sequenom iPlex platform by BioServe (Beltsville, MD, USA). In the two infant populations, we used χ^2 analyses (dominant and recessive modeling; SigmaPlot 13.0) to test for associations between *MARCO* genotypes and RSV disease severity. We assessed potential confounding of demographic variables in the relationships between *MARCO* genotype and RSV disease severity using an additive model for multiple logistic regressions. Statistical significance in these and all other comparisons was accepted at $P < 0.05$.

3. Results

3.1. Phenotypic Characterization of RSV Disease in Inbred Mice

We developed a genetic model of RSV disease by infecting intranasally 30 strains of mice. Inflammation was assessed in BALF by measuring total protein concentration and counting inflammatory and epithelial cells 1 and 5 days PI. The time courses of inflammation and injury phenotypes indicated early (acute) and late phase responses in all of the strains tested. Relative to vehicle controls, mean numbers of total cells, polymorphonuclear leukocytes (PMNs), epithelial cells, and total protein in BALF of infected mice were significantly increased 1 day PI and declined 5 days PI in the majority (>50%) of strains (representative strains, Fig. 1a; all strains, Suppl. Table S2). Numbers of BALF macrophages, lymphocytes, and monocytes (representative strains, Fig. 1b; all strains, Suppl. Table S2) peaked at 5 days PI in the majority of strains. The differences in kinetics may reflect the sequential contributions of the innate and acquired immune systems in response to infection as others have found [e.g. (Kok et al., 2012; Stoppelenburg et al., 2013)]. Qualitative inspection of lung histopathology sections was consistent with BALF inflammation phenotypes (Fig. 1c). Mucus cell metaplasia is a clinical feature of RSV disease, and we found the mean amount of intraepithelial cell mucus (Fig. 1d; Suppl. Table S2) and lung RSV-N mRNA expression (Suppl. Table S2) were greatest 1 day PI in 59% and 70% of the strains, respectively.

We also found statistically significant inter-strain variation in the peak of each RSV disease phenotype. That is, significantly smaller numbers of inflammatory cells and other indicators of injury (mild disease) were found in a subset of strains (e.g. C3H/HeJ) compared to others with severe disease (e.g. BALB/cByJ) (Fig. 2a–d; Suppl. Table S2; Suppl. Fig. S1). Heritability estimates of RSV disease phenotypes ranged from 47.6% (BALF protein, 1 day PI) to 85.7% (intraepithelial mucus, 1 day PI) (Suppl. Table S2). To better understand mechanisms of response to RSV infection, we tested for correlation of disease phenotypes. Pearson's correlation analyses of RSV disease phenotypes among 30 strains found that responses 1 day PI did not correlate with responses 5 days PI (data not shown). When maximum responses for each parameter were compared, few were significantly correlated (Fig. 1e; Fig. 2). Interestingly, RSV-N mRNA expression was not correlated with any response phenotype, a finding consistent with lack of correlation we found between RSV disease severity and RSV titers in infected children (Caballero et al., 2015). Large inter-strain variation and relatively high heritability of distinct disease phenotypes suggests the mouse model of response to RSV infection is multi-genic and mimics the variability of RSV disease severity found in human populations.

3.2. Identification of QTLs and Gene Candidates for RSV Disease Phenotypes

Because the phenotypic responses to RSV infection were largely not correlated, we reasoned that the phenotypes may have some QTLs in common, but likely also have unique QTLs. Therefore, we used GWA mapping to identify QTLs for each phenotype across the entire inbred strain data set. Using the maximum mean response phenotypes for each strain, mapping with SNPster identified significant ($-\mathrm{Log}_{10}$ $P > 6.6$) QTLs for RSV-induced changes in BAL monocytes (chromosomes 1 and 17; Fig. 3a, Table 1) and PMNs (chromosomes 3 and 8; Table 1), and the first PC (chromosomes 4, 11, and 13; Table 1). Suggestive QTLs ($-\mathrm{Log}_{10}$ $P > 6.0$) were also found for intraepithelial mucus content (chromosomes 7 and 15), BALF total protein concentration (chromosomes 9 and 19), and lung RSV-N mRNA expression (chromosomes 1 and 11) (Table 1). Importantly, all QTLs were also identified using FastMap (data not shown). GWA mapping of other RSV response phenotypes with SNPster did not identify significant or suggestive QTLS, or were not confirmed with FastMap.

To further investigate genetic contributions to RSV disease phenotypes we searched the MPD for informative SNPs in susceptibility gene candidates within significant and suggestive QTLs, and whether they

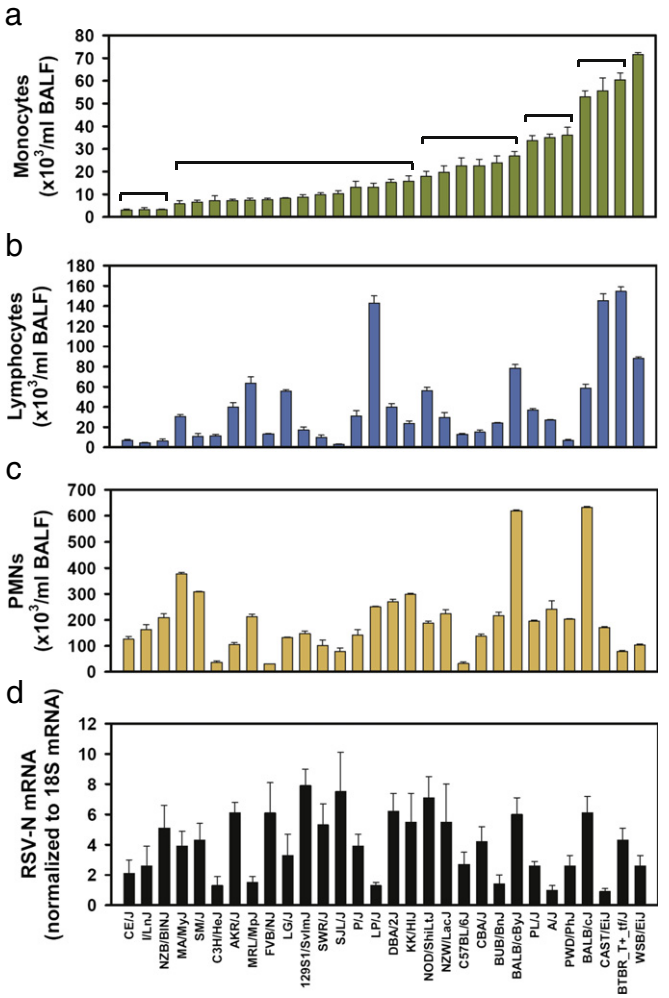

Fig. 2. Lung disease phenotypes in mice infected with RSV. Maximum numbers of BALF monocytes (a), lymphocytes (b), and PMNs (c), and RSV-N mRNA expression (d) in lung homogenates. Bars, means ± SEM (n = 6–12/group). Horizontal brackets (monocytes) indicate means are not significantly ($P < 0.05$) different from each other (1-way ANOVA and Student-Newman-Keuls comparisons of means).

associated with respective disease phenotypes. Genes were chosen for investigation if they had biological plausibility for a role in RSV disease and if the minor allele of candidate SNPs were present in ≥10% of the phenotyped inbred strains. Eleven gene candidates were identified in 9 QTLs that met these criteria and also contained SNPs that associated with differential susceptibility to an RSV disease phenotype (Table 2),

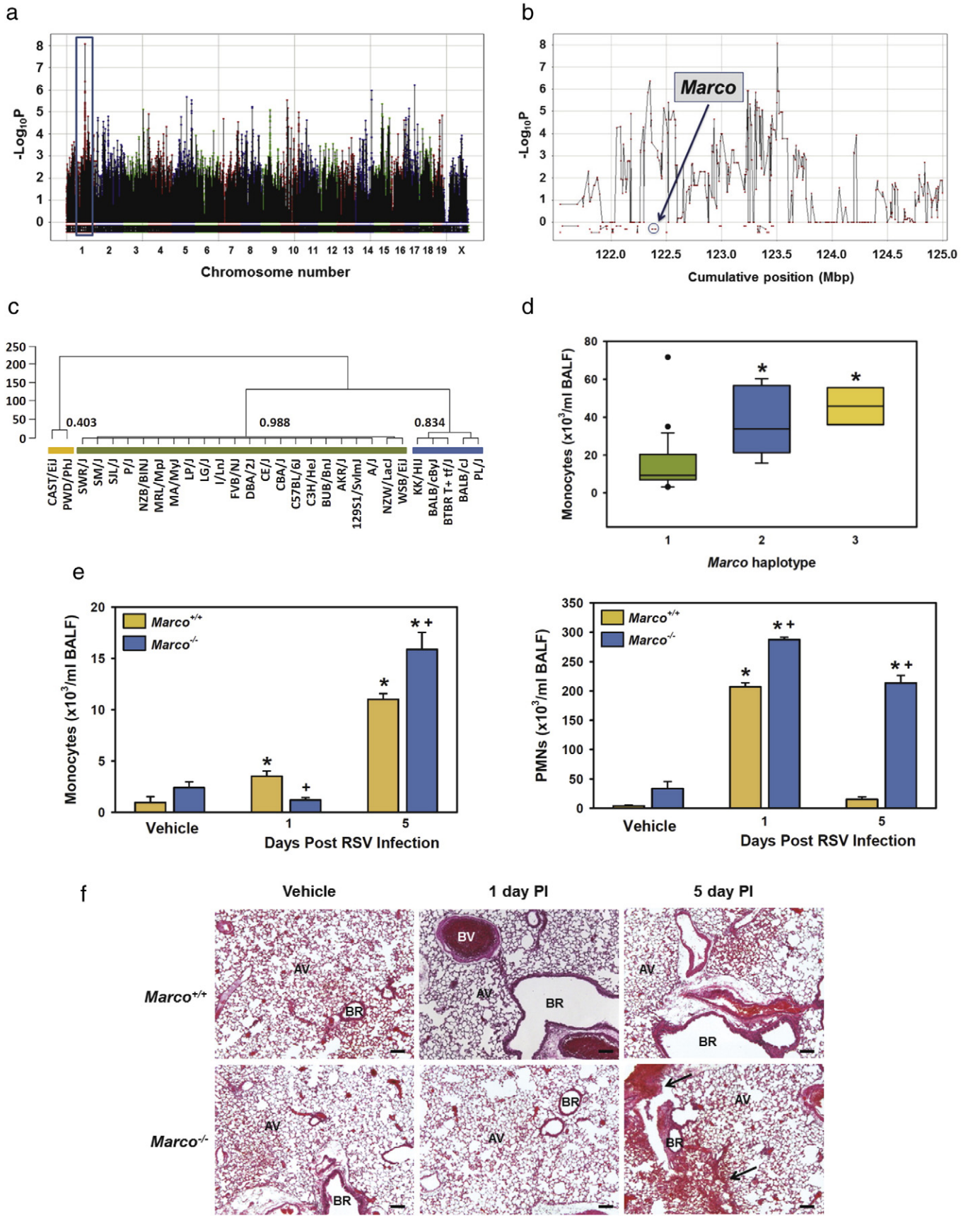

thus supporting a potential role for these genes in murine RSV disease severity.

We focused initially on the chromosome 1 QTL for monocyte inflammation to validate gene candidates because this QTL (~1.299 Mb) had the greatest GWA $-\text{Log}_{10}$ P value (Table 2). The scavenger receptor gene *Marco* is located in the QTL (Fig. 3b) and is in linkage disequilibrium (LD) with the SNP that has the highest −Log P value in the QTL, and human *MARCO* is upregulated in children infected with RSV [i.e. biological plausibility (Fjaerli et al., 2006)]. Hierarchical clustering of *Marco* SNPs identified 3 major haplotypes in the strain panel (Fig. 3c; Suppl. Table S3). Mean numbers of RSV-induced BAL monocytes in strains from *Marco* haplotypes 2 and 3 were significantly greater than those in strains from wild-type haplotype 1 (Fig. 3d). Potentially functional, informative SNPs are located in *Marco*, including the non-synonymous coding SNP rs30741725 (A/T) that causes a threonine to serine substitution at the 476 amino acid residue in exon 17. Significantly increased numbers of BAL monocytes and lymphocytes 5 days PI were found in strains of mice with the minor T allele for this SNP compared with strains that have the major A allele (Table 2; Suppl. Fig. S2A and S2B). The majority of strains with the T allele have *Marco* haplotypes 2 or 3. The rs30741725 A/T SNP is in LD with other SNPs in the *Marco* haplotype, so a definitive role for this SNP in differential RSV responsiveness requires further investigation. There are 5 other protein-coding genes in the QTL with *Marco*, but none have known biological plausibility for the RSV response phenotypes or do not meet criteria for further study (stated above).

Table 1
Quantitative trait loci (QTL) type, genomic location, and maximum $-\text{Log}_{10}$ P value identified by haplotype association mapping using SNPster and FastMap in 30 inbred strains of mice.

Phenotype	Chromosome	QTL type	Genomic location (Mb)	Max $-\text{Log}_{10}$ P
Monocytes	1	Significant	122.292051–123.591461	8.0764
	17	Significant	63.717121–63.851568	6.2074
Lymphocytes	1	Suggestive	52.516061–52.626962	4.2831
	4	Suggestive	154.164390–154.306615[a]	4.5528
	11	Suggestive	32.132950–33.743190[a]	4.6383
PMNs	3	Significant	90.189278–92.304415	7.0324
	8	Significant	116.222735–121.343307	6.1851
Mucus	7	Suggestive	130.318155–130.535201	4.2492
	15	Suggestive	10.421905–11.278506	4.3576
Protein	9	Suggestive	99.381216–99.610367	5.8803
	19	Suggestive	42.164991–42.683021	5.2600
RSV N	1	Suggestive	92.939552–93.424360	4.5088
	1	Suggestive	151.202928–152.311735	4.8599
	11	Suggestive	116.303373–116.468685	4.5465
PC 1	4	Significant	153.237964–154.148432[a]	6.6645
	11	Significant	31.520635–32.654798[a]	6.8655
	13	Significant	60.210819–60.772421	6.7123

PC1, first principal component.
[a] Overlaps with another QTL.

3.3. Genetic Deletion of Marco Modifies RSV-induced Pulmonary Inflammatory Response

We further investigated the role of *Marco* on RSV disease severity by infecting $Marco^{+/+}$ and $Marco^{-/-}$ mice with RSV. Relative to vehicle controls, RSV increased BALF monocytes in $Marco^{+/+}$ and $Marco^{-/-}$ mice, and numbers of monocytes in $Marco^{-/-}$ mice were slightly lower compared to $Marco^{+/+}$ mice 1 day PI, during the development of the monocyte response. However, numbers were significantly greater in $Marco^{-/-}$ mice compared to those in $Marco^{+/+}$ mice at the peak of the response (5 days PI; Fig. 3e, left). Mean numbers of PMNs were also significantly increased in $Marco^{+/+}$ and $Marco^{-/-}$ mice 1 day PI, but were significantly greater in $Marco^{-/-}$ mice compared to $Marco^{+/+}$ mice, and remained significantly elevated at 5 days PI (Fig. 3e, right). BALF inflammation phenotypes were consistent with lung histopathology sections from $Marco^{+/+}$ and $Marco^{-/-}$ mice (Fig. 3f). No significant genotype effects were found for other RSV BALF phenotypes (data not shown). Lack of resolution of the PMN response in $Marco^{-/-}$ mice is consistent with the hypothesis that inflammatory cell clearance is impaired in these mice.

3.4. Functional Assessment of the Human MARCO Promoter

Based on our GWA investigation and identification of *Marco* as a gene candidate for differential RSV disease severity in the mouse, we queried dbSNP (build 129, 2008) to identify potentially relevant SNPs in human *MARCO* based on functional annotation. A missense SNP (rs61732822, Asp511Glu) in the scavenger receptor cysteine rich (SRCR) domain of exon 17 (similar to that found in mouse *Marco*), is predicted by SIFT (sift.jcvi.org) to have deleterious consequences, but the 1000 genomes project phase 1 (www.1000genomes.org) indicates the alternate allele frequency of 0.055 is too low to study in our populations of children with RSV-induced bronchiolitis. We then asked whether the *MARCO* promoter contains polymorphic regions that might alter transcriptional efficiency. We consecutively deleted sections of the promoter from −1388 to −71 and probed for transcriptional activity using luciferase reporter constructs. We identified a region close to the transcription start site (−300 to −71) that, when deleted, significantly reduced transcriptional activity (Fig. 4a). We then screened commercially available DNA samples (n = 40; Coriell Institute, Camden, NJ) for SNPs in the *MARCO* promoter region. Forty subjects (20 European, 20 African-American) were chosen to provide a detection rate of 98% for SNPs present in as little as 5% of the population. The screen identified a SNP (rs1318645, −156 C/G; Suppl. Fig. S3) that contained a putative antioxidant response element for NRF2 [C allele, position weight matrix (PWM) score = 10.9; G allele, PWM score = 7.5]. Mutation of the −156 site from C (wild type) to G completely reduced luciferase activity to that of the pGL3 basic vector (Fig. 4b).

Polymorphic and ARE deletion constructs cloned in BEAS-2B epithelial cells were also assessed for transcriptional activity following RSV infection. Robust *MARCO* activation was found 3, 6 and 24 h PI, and mutation from C to G at the −156 site reduced activity approximately 50% at 6 h PI, and constructs with ARE deletion caused similar reduction in activity (Fig. 4c). At 24 h PI, luciferase activity in constructs with ARE deletion was reduced by 50% compared to that of wild type −300C

Fig. 3. Genome-wide haplotype association map of BALF monocytes in 30 mouse strains infected with RSV and *Marco* haplotype clustering and monocytic inflammatory response to RSV infection. (a) Manhattan plot for maximum mean BALF monocytes in 30 strains of mice. X axis, chromosome number and cumulative genomic position; Y axis, $-\text{Log}_{10}$ P values. The rectangle on chromosome 1 identifies a locus significantly associated with RSV-induced monocyte infiltration. (b) Detailed view of the chromosome 1 QTL for monocyte response to infection. The gene *Marco* is indicated within the locus. (c) Hierarchical clustering of 29 mouse strains based on 87 *Marco* SNPs (http://phenome.jax.org/SNP). Numbers represent uncertainty in genotype changes after clustering (Φ), where Φ = 1 − cluster entropy / crude entropy. If, after clustering, all strains in the cluster have the same genotype then Φ = 1; if Φ = 0, the genotype distribution within the cluster is as variable as the genotype distribution across all strains. (d) Box plots of numbers of BALF monocytes following RSV infection in strains with *Marco* haplotypes 1, 2, and 3. The boundary of the box closest to zero indicates the 25th percentile, a line within the box marks the median, and the boundary of the box farthest from zero indicates the 75th percentile. Error bars above and below the box indicate the 90th and 10th percentiles. Outlying points are shown for haplotype 1. *P < 0.05 versus *Marco* haplotype 1 (1-way ANOVA and Student-Newman-Keuls comparisons of means). (e) Differential pulmonary disease phenotypes after RSV infection in $Marco^{+/+}$ and $Marco^{-/-}$ mice. Means (±SEM) of monocytes (left) and PMNs (right) recovered in BALF after vehicle or RSV infection. *P < 0.05 versus vehicle; $^{+}$P < 0.05 versus $Marco^{+/+}$ mice (3-way ANOVA with Student-Newman-Keuls comparisons of means). (f) Pulmonary pathology 1 and 5 days following vehicle control or RSV infection in $Marco^{+/+}$ and $Marco^{-/-}$ mice. Arrows indicate areas of increased airway inflammation and bronchial epithelial proliferation (hyperplasia). AV = Alveoli, BR = bronchus or bronchiole, BV = blood vessel. Bar = 100 μm.

Table 2
Associations of candidate gene functional single nucleotide polymorphisms (SNPs) with RSV-induced lung inflammation phenotypes.

Phenotype	QTL chromosome	Gene symbol	SNP rs ID	Location (Mb)	SNP function	Major allele, mean ± SEM, N	Minor allele, mean ± SEM, N	P-value
Monocytes	1	*Marco*	rs30741725	120.474787	CNSyn, Thr476Ser	A, 38.4 ± 8.8; 19	T, 14.5 ± 2.7; 10	<0.001
Lymphocytes	11	*Mpg*	rs26841220	32.231754	CNSyn, Arg254Gln	G, 28.9 ± 6.1; 24	A, 80.6 ± 22.6; 6	0.004
PMNs	3	*Lor*	rs31130301	91.885023	CNSyn, Gly293Arg	G, 134.3 ± 18.8, 16	C, 275.2.5 ± 50.4; 12	0.005
	8	*Adamts18*	rs37229383	116.233617	CNSyn, Gly957Arg	G, 226.1 ± 34.1; 21	C, 116.2 ± 24.3; 7	0.046
Mucus	7	*Aqp8*	rs32822168	123.462409	5′ UTR	A, 1.13 ± 0.3; 24	C, 0.6 ± 0.2; 3	NS
Protein	19	*Sfrp5*	S19-42272711	42.272711	3′ UTR	C, 342.1 ± 32.3; 19	T, 222.2 ± 13.4; 7	0.042
RSV-N	1	*Ramp1*	rs47959958	91.206647	3′ UTR	A, 5.6 ± 0.3; 14	G, 2.3 ± 0.3; 12	<0.001
		Espnl	rs48467891	91.320153	CNSyn, Gly406Ser	G, 4.8 ± 0.5; 19	A, 2.8 ± 0.4; 11	0.011
		Per2	rs32164384	91.445550	CNSyn, Ser172Thr	G, 4.7 ± 0.4; 21	C, 2.4 ± 0.4; 9	0.003
	1	*Ptgs2*	rs32559831	151.948631	Intronic	A, 5.1 ± 0.5; 14	T, 2.5 ± 0.4; 10	<0.001
	11	*Rhbdf2*	rs29403288	116.471777	3′ UTR	C, 4.9 ± 0.4; 20	T, 2.4 ± 0.5; 7	0.005
PC1	11	*Mpg*	rs26841220	32.231754	CNSyn, Arg254Gln	G, −0.50 ± 0.3; 24	A, 1.99 ± 0.1; 6	<0.001

Adamts18, a disintegrin-like and metallopeptidase (reprolysin type) with thrombospondin type 1 motif, 18; *Aqp8*, aquaporin 8; CNSyn, non-synonymous coding SNP; *Espnl*, espin-like; *Lor*, loricrin; *Marco*, macrophage receptor with collagenous structure; *Mpg*, *N*-methylpurine-DNA glycosylase; *Per2*, period circadian clock 2; PC1, first principal component; *Ptgs2*, prostaglandin-endoperoxide synthase 2; *Ramp1*, receptor (calcitonin) activity modifying protein 1; *Rhbdf2*, rhomboid 5 homolog 2 (*Drosophila*); *Sfrp5*, secreted frizzled-related sequence protein 5; UTR, untranslated region.

constructs (Fig. 4c). Transcription activity was close to basal levels 48 and 72 h PI (data not shown).

Gel shift analysis showed reduced NRF2 specific binding in the presence of the variant G allele in the potential ARE (Fig. 4d), suggesting binding efficiency is altered at this polymorphic site. Overall binding was increased with the G allele, suggesting additional factors may bind this regulatory locus.

3.5. Role of MARCO rs1318645 in RSV Disease Severity

Next we asked whether the *MARCO* SNP rs1318645 that caused reduced MARCO gene expression in vitro (see above) associated with increased risk of severe RSV disease in populations of infected infants from our prospective case-control study (Ciencewicki et al., 2014; Caballero et al., 2015). Demographic characteristics are described elsewhere (Caballero et al., 2015). Genotyped (Fig. 5a) infants with mild and severe infection had combined allelic frequencies (Suppl. Table S4) similar to those published previously (http://www.1000genomes.org/). We were unable to successfully genotype 39 infants in the first population and 25 in the second population, and there was no association of unsuccessful genotyping between cases and controls. Allelic frequencies satisfied Hardy-Weinberg equilibrium ($P = 0.369$) and, although admixture was present we found no evidence of bias due to population stratification (i.e. stratification was not predictive of differential RSV disease severity). χ^2 analysis of RSV disease severity found the rs1318645 C/G polymorphism was associated with increased risk of severe RSV disease (Fig. 5b; $\chi^2 = 5.15$, $P = 0.053$). The association was largely attributed to GG risk effect (recessive model) where infants homozygous for the G allele were at significant risk of developing severe RSV disease compared to CC and CG genotypes (Suppl. Table S5). In a second, independent population, we found the *MARCO* rs1318645 C/G allele was again associated with RSV disease severity in infected infants (Fig. 5b; $\chi^2 = 8.15$, $P = 0.017$) and similar to the first population, the association was driven by GG genotype (Suppl. Table S5). Association of the *MARCO* rs1318645 C/G allele with RSV disease severity in the combined population was significantly strengthened compared to either population alone (Fig. 5b; $\chi^2 = 10.34$, $P = 0.003$), and the homozygous GG genotype conferred approximately 62% greater risk of severe RSV disease compared to CC and CG genotypes (Suppl. Table S5). Using multiple logistic regression we found the *MARCO* rs1318645 C/G allele was associated with increased risk of severe RSV disease (unadjusted OR: 1.654, 95% CI: 0.98, 2.58). After adjusting for gender, socioeconomic status, and breastfeeding the SNP remained associated with severe RSV disease (adjusted OR: 1.684, 95% CI: 1.03, 3.15). Similar outcomes were found in the second population (unadjusted OR: 1.744, 95% CI: 1.10, 2.44; adjusted OR: 1.82, 95% CI: 1.13, 2.56) and in the combined populations (unadjusted OR: 1.615, 95% CI: 1.24, 2.35; adjusted OR: 1.676, 95% CI: 1.28, 2.45).

4. Discussion

The impact of RSV disease, particularly in vulnerable infants, remains a global public health concern (Lozano et al., 2012). Unfortunately, no RSV vaccines are approved for clinical use. Therefore, it is critical to identify host risk factors that lead to development of prevention and intervention strategies to reduce risk of RSV disease morbidity and mortality, as well as asthma incidence because RSV disease has been identified as a predisposing risk factor (Dakhama et al., 2005; Edwards et al., 2012; Gelfand, 2012; Feldman et al., 2015). Our study used genome-wide association analyses of RSV disease parameters that model human disease to identify biologically plausible susceptibility gene candidates, including *Marco*. Moreover, a missense loss of function polymorphism in the human *MARCO* homolog also associated with severe RSV disease in two populations of infected infants, and illustrates the utility of a genetic mouse model for understanding human disease. Importantly, this study provides additional genetic insight that may lead to a means to identify individuals at risk for severe RSV disease.

Considerable evidence has suggested that genetic background is an important host determinant of RSV disease severity, but full characterization of susceptibility genes for this complex disease remains unclear. Previous genetic investigations of human RSV disease have questioned whether polymorphisms in gene candidates associate with innate and acquired immune responses to infection and have provided some understanding of susceptibility factors. Gene candidates in these studies were chosen because of prior knowledge about biological plausibility. We comprehensively characterized RSV disease phenotypes in a large panel of inbred strains representing genetic diversity that is present in the mouse genome. We found significant variation and robust heritability in each RSV disease phenotype between the strains. However, relatedness between maximum response phenotypes was minimal, suggesting multiple genetic pathways likely contribute to the responses.

Anh and Desmecht (2006) reported that pneumonia virus of mice (PMV, the murine form of RSV) infection in a panel of 6 strains caused strain-specific histopathologic inflammatory effects, decreased body weight, and changes in pulmonary function particularly 5–7 days PI. The studies are not directly comparable because mice were infected with different viruses and late phase PI times investigated, but the inter-strain variation in phenotypes is consistent with our findings. Others (Stark et al., 2002) compared RSV infection in 8 inbred strains and found significant inter-strain variation in infectivity at 4 days PI, but histopathologic changes were minimal and cellular effects were

discordant with the magnitude of infection likely due to the time point when acute virus effects on histopathology were no longer present.

We leveraged extensive genetic diversity among the 30 strains of mice to perform GWA of multiple RSV disease phenotypes and thus were not guided a priori by hypotheses about the role of specific genes. Significant and suggestive QTLs were identified for inflammatory cells, intraepithelial cell mucus, and RSV N mRNA expression. Several genes that may contribute to viral response, pulmonary inflammation, and cytokine trafficking were found within the identified QTLs [e.g. *Ptgs2* (Obata et al., 2013), *Ramp1* (Li et al., 2014), *Rhbdf2* (Issuree et al., 2013)], and putative functional SNPs in the genes associated with differential RSV disease phenotypes among the strains. SNPs in other QTL genes strongly associated with disease phenotypes and, while little is known about their function in infectious disease, they may be important targets for future investigation of their roles in RSV disease progression. We also found significant QTLs using the first PC as an RSV disease index. Two of these QTLs overlapped those found for lymphocytes, and suggests that further investigation of genes within the QTLs could provide greater understanding of disease susceptibility. Future GWA investigations using PC analyses may provide additional insight to disease pathogenesis beyond using single phenotypes. Interestingly, genome-wide linkage analyses of RSV infectivity in back-cross and F_2 populations derived from C57BL/6J and AKR/J mice by Stark et al. (2010) identified a QTL on chromosome 6 that associated with increased susceptibility to infection, though disease phenotypes were not presented. While GWA in the present investigation identified suggestive QTLs on chromosomes 1 and 11 for RSV-N mRNA expression, none were detected on chromosome 6. Differences in study design (e.g. haplotype mapping with many strains versus linkage analysis with 2 strains, PI time differences) may have contributed to this discrepancy.

We focused on the gene candidate *Marco*, which was identified by GWA for monocytes, and has been shown previously to have protective effects in the lung following inhalation of particulate matter, exposure to ozone, and bacterial infection (Arredouani et al., 2005; Dahl et al., 2007; Thakur et al., 2008; Thakur et al., 2009; Ghosh et al., 2011). *MARCO* gene expression was also upregulated in children infected with RSV (Fjaerli et al., 2006). Our hypothesis that *Marco* contributes to defense against RSV-induced pulmonary inflammation was supported by two lines of evidence. First, strains of mice with a *Marco* haplotype containing the T allele of missense coding SNP rs30741725 were at greater risk of developing more severe RSV disease compared to strains with the wild type A allele. Second, numbers of BALF monocytes and PMNs were significantly increased in *Marco*$^{-/-}$ mice compared to *Marco*$^{+/+}$ mice. The mechanism through which *Marco* modulates the inflammatory response to RSV is not completely understood. We initially hypothesized that Marco has a direct role in clearing RSV from the airways, perhaps binding the virus for internal degradation by macrophages. To test this hypothesis, we infected with RSV lung macrophages isolated from *Marco*$^{+/+}$ and *Marco*$^{-/-}$ mice but found no differences in infectivity, with and without co-culturing with epithelial cells (data not shown). Marco also has an important role in clearance of apoptotic cells (Rogers et al., 2009; Getts et al., 2014), and recent studies have targeted Marco receptors with immune-modifying particles to resolve monocytic inflammation (Getts et al., 2014). It is plausible that

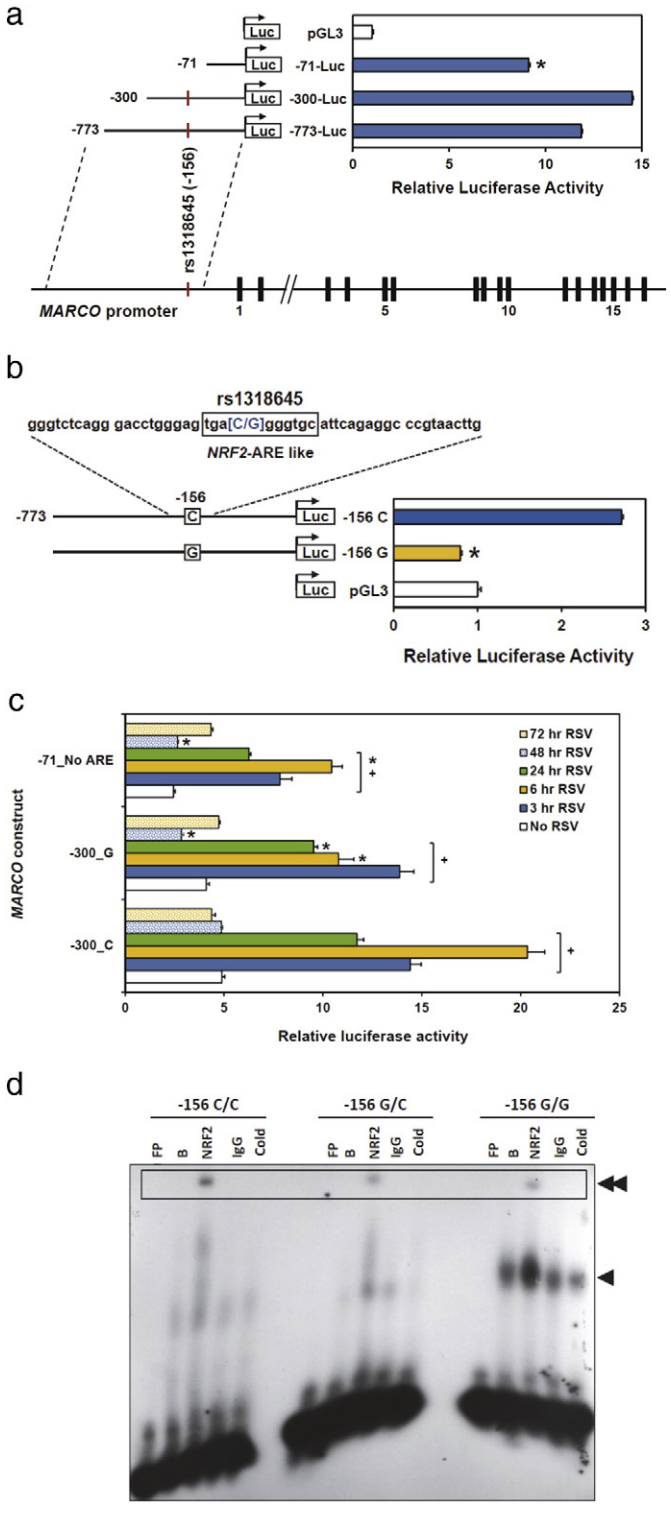

Fig. 4. Effect of a genetic polymorphism on in vitro *MARCO* promoter activity. (a) Deletion analysis of the *MARCO* promoter compared to pGL3 basic vector. *P < 0.05 versus −300-Luc; group sizes = 4. (b) Mutagenesis analysis of the *MARCO* rs1318645 variant (−156G) compared to pGL3 basic vector. Bars (means ± SEM) represent luciferase activity in basic vector, control −156 C allele, and mutant −156 G constructs. Flanking sequence for *MARCO* rs1318645 is shown at top with the NRF2 response element boxed. *P < 0.05 versus −156 C (P = 0.001); group sizes = 4. Statistical analyses, one-way ANOVA and Student-Newman-Keuls comparisons of means. (c) Luciferase activity of RSV infected *MARCO* reporter constructs. *MARCO* promoter constructs were transiently transfected and cells infected with RSV (MOI of 4). Bars (means ± SEM) represent luciferase responses after no RSV (control) or 3–72 h post-infection (PI). Cells were harvested 3–72 h PI and relative luciferase activity assessed. *P < 0.05 versus RSV-infected −300_C (WT); $^{+}$P < 0.05 versus No RSV control; group sizes = 6. Statistical analyses, 2-way ANOVA and Student-Newman-Keuls comparisons of means. (d) Gel shift analysis of *MARCO* promoter variants. Gel shift analysis of *MARCO* −156 CC (wild type), GC and GG (variant) oligos show increased overall binding in the presence of the G allele. Incubation with NRF2 antibody shows reduced MARCO:NRF2 specific binding with the variant G allele. This suggests the *MARCO* G allele affects efficient binding to the NRF2 ARE site, and may alter transcriptional activity. A representative gel shift is shown; group sizes n = 3. Single arrowhead, overall binding; double arrowhead, *MARCO*:NRF2 specific binding. FP is free radiolabeled probe, B is bound, NRF2 is NRF2 antibody, IgG is control serum, and Cold is competition without antibody (40×).

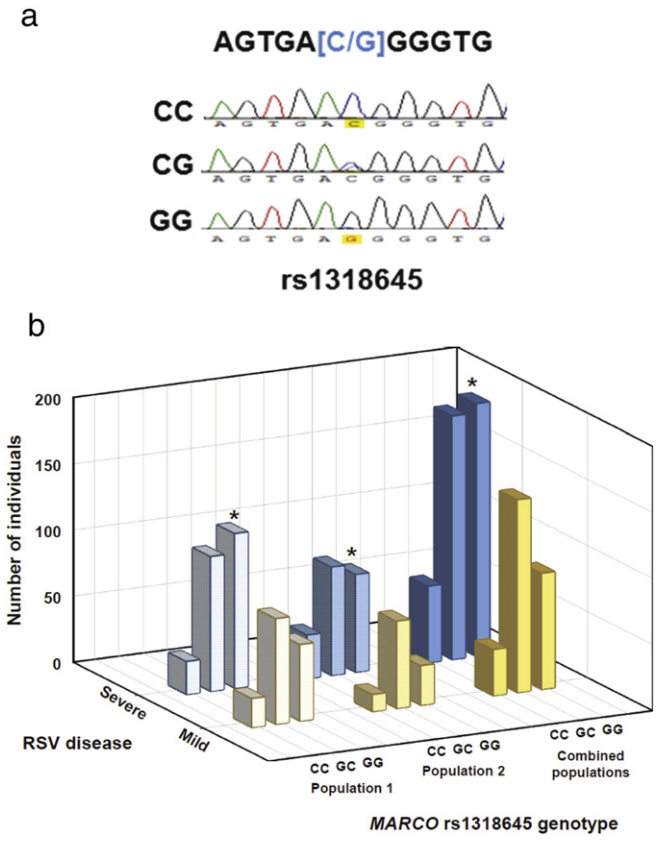

Fig. 5. Effect of the *MARCO* rs1318645 C/G polymorphism on human RSV disease severity. (a) Representative electropherograms of the *MARCO* promoter and putative NRF2 binding site with the rs1318645 C/G polymorphism. (b). Role of *MARCO* rs1318645 C/G in disease severity among two populations of infants infected with RSV. Infants with mild or severe RSV disease were genotyped for the MARCO SNP and determined to be homozygous for the major (C) or minor (G) allele, or heterozygous. χ^2 analysis of disease severity among the three genotypes was done independently for both populations and the two combined. *P < 0.05 versus the CC and CG genotypes.

loss of function mutations in *Marco* compromise clearance of monocytes and apoptotic cells which leads to accumulation of these cells in the airways, further contributing to RSV disease pathology. Impaired resolution of the inflammatory response to RSV infection and more severe disease in $Marco^{-/-}$ mice compared to $Marco^{+/+}$ mice is consistent with this hypothesis.

It is important to note that *Marco* does not account for all of the monocyte inflammation caused by RSV infection. Targeted deletion of *Marco* significantly increased susceptibility to some RSV-induced phenotypes but did not account for all of the genetic variation identified by the strain screen. The background strain (C57BL/6 in this model, a moderate responder to RSV) likely contributes to part of this difference as the choice of background can influence the effect of targeted deletion in mice [e.g. (Baleato et al., 2008; Leontyev et al., 2012)]. Perhaps more importantly, other QTLs were also identified by the GWA and gene candidates within them also contribute to the genetic component of the phenotype. Further investigation of these QTLs should provide additional insight to the genetic contribution to RSV disease susceptibility.

Because *Marco* had an important role in modulating the inflammatory response elicited by RSV, we sought to determine whether human *MARCO* was also important in RSV disease. We initially queried whether the *MARCO* rs1318645 −156 C/G SNP caused loss of function because it was located in an ARE proximal to the transcription start site. Others had found that the transcription factor NRF2, which binds to AREs to increase gene transcription, had a role in *Marco* expression in mice (Harvey et al., 2011; Bonilla et al., 2013). We showed previously that murine *Marco* bears a potentially functional ARE for Nrf2 binding (−940 region, PWM score = 8.9) in a model of neonate acute lung injury (Cho et al., 2012). In the present study, we found that deletion of the ARE and mutating the −156 site in an ARE in human *MARCO* also significantly attenuated gene expression as well as *MARCO*:NRF2 specific binding. Moreover, deletion of the ARE also significantly reduced expression of *MARCO* in cells infected with RSV thus suggesting an important role for the ARE and the rs1318645 −156 C/G SNP in *MARCO* function, basally and in response to viral infection. This is supported by our previous study in which increased lung injury and inflammation were found in *Nrf2* deficient mice compared to wild type mice after RSV infection (Cho et al., 2009).

We further investigated the role of *MARCO* in human RSV disease by asking whether the missense *MARCO* rs1318645 G allele was more prevalent in infected children with severe disease. In two independent populations, infected children homozygous for the rs1318645 G allele were more likely to have severe RSV disease than children who were heterozygous or wild-type for the C allele. The significance of the risk effect was increased when the populations were combined. The *MARCO* promoter SNP increased the risk for severe RSV disease by approximately 62%. A previous investigation tested whether 9 non-synonymous coding variants or tag SNPs in *MARCO* associated with chronic obstructive pulmonary disease and found no association, although one of the SNPs (rs41279766) associated with the risk of sepsis (Thomsen et al., 2013). Another study found tag SNPs associated with increased risk of pulmonary tuberculosis, while another was associated with resistance (Bowdish et al., 2013), thus the role of *MARCO* in this disease is not clear.

A caveat for this investigation is that, although we tested for a number of potential co-factors in our studies, it is possible that other confounders or unmeasured environmental factors may contribute to the differences in disease severity that associated with the *MARCO* rs1318645 G allele. For example, gender has been found to be important in susceptibility to some lung diseases in mouse models (Carey et al., 2007; Cabello et al., 2015). In the present study, we used only male mice. Although we are not aware of sexual dimorphism effects in RSV disease, male and female mice respond differentially to influenza A infection (Larcombe et al., 2011). Another important RSV disease phenotype is airways hyperreactivity (Yoo et al., 2013). We chose to focus the present studies on the inflammation and injury responses to RSV infection, but investigations into the genetic basis of susceptibility to RSV-induced airway hyperreactivity may also identify important susceptibility genes. It is also feasible that different strain distribution patterns may be found with a different line of RSV. Lukacs et al. (2006) found that different strains of RSV of the same antigenic subgroup may cause different RSV-induced phenotypes in BALB/cJ mice, and it is possible that other strains also respond differently to multiple RSV lines. Finally, it is important to emphasize that, while the rs1318645 SNP associated significantly with RSV disease in these populations, other gene polymorphisms also contribute to susceptibility, including myxovirus (influenza virus) resistance 1 (*MX1*) (Ciencewicki et al., 2014) and toll-like receptor 4 (*TLR4*) (Caballero et al., 2015), and interactions between these and other, unknown, genetic contributions remain to be clarified. It is likely that continued investigation of gene candidates identified with GWA for all of the phenotypes in the mouse model will add to our understanding of RSV disease susceptibility.

In conclusion, this translational investigation identified gene candidates, including *Marco*, for host susceptibility to multiple phenotypes of RSV disease in mice that closely mimic human disease, and a polymorphism in human *MARCO* associated with increased risk of RSV disease severity in infants. Continued investigation of the genetic basis of differential susceptibility to RSV disease may lead to a panel of informative SNPs to identify children who are at risk for disease severity. In the absence of an RSV vaccine, these individuals could be treated prophylactically with an RSV monoclonal antibody to prevent infection and sequelae associated with severe disease such as childhood asthma.

Funding Sources

Research related to the manuscript was supported by the Intramural Research Program of the National Institutes of Health, NIEHS (Z01 ES 100557).

Conflict of Interest Statement

The authors declare no conflicts of interest or competing financial interests.

Author Contributions

S.R.K., M.H., H.C., J.M., and F.P.P. designed the study. M.G.C., P.L.A., M.E.S., and F.P.P. coordinated the infant population studies. M.H., L.M.-D., and W.G. bred and maintained the mice and performed the experiments. M.H., T.W., K.C.V., Z.R.M., L.K., D.B.P., M.S., C.W., O.S., X.W., D.A.B., F.P.P., and S.R.K. contributed to data analysis and interpretation. M.H., H.C., and S.R.K. drafted the manuscript. All authors edited the manuscript.

Acknowledgments

Drs. Michael Fessler and Donald Cook at the NIEHS provided excellent critical review of the manuscript.

Appendix A. Supplementary Data

Supplementary data to this article can be found online at http://dx.doi.org/10.1016/j.ebiom.2016.08.011.

References

Anh, D.B.F.P., Desmecht, J.M., 2006. Differential resistance/susceptibility patterns to pneumovirus infection among inbred mouse strains. Am. J. Phys. Lung Cell. Mol. Phys. 291, 426–435.

Arredouani, M., Yang, Z., Ning, Y., Qin, G., Soininen, R., Tryggvason, K., Kobzik, L., 2004. The scavenger receptor MARCO is required for lung defense against pneumococcal pneumonia and inhaled particles. J. Exp. Med. 200, 267–272.

Arredouani, M.S., Palecanda, A., Koziel, H., Huang, Y.C., Imrich, A., Sulahian, T.H., Ning, Y.Y., Yang, Z., Pikkarainen, T., Sankala, M., et al., 2005. MARCO is the major binding receptor for unopsonized particles and bacteria on human alveolar macrophages. J. Immunol. 175, 6058–6064.

Baleato, R.M., Guthrie, P.L., Gubler, M.C., Ashman, L.K., Roselli, S., 2008. Deletion of CD151 results in a strain-dependent glomerular disease due to severe alterations of the glomerular basement membrane. Am. J. Pathol. 173, 927–937.

Benton, C.S., Miller, B.H., Skwerer, S., Suzuki, O., Schultz, L.E., Cameron, M.D., Marron, J.S., Pletcher, M.T., Wiltshire, T., 2012. Evaluating genetic markers and neurobiochemical analytes for fluoxetine response using a panel of mouse inbred strains. Psychopharmacology 221, 297–315.

Bonilla, D.L., Bhattacharya, A., Sha, Y., Xu, Y., Xiang, Q., Kan, A., Jagannath, C., Komatsu, M., Eissa, N.T., 2013. Autophagy regulates phagocytosis by modulating the expression of scavenger receptors. Immunity 39, 537–547.

Bowdish, D.M., Sakamoto, K., Lack, N.A., Hill, P.C., Sirugo, G., Newport, M.J., Gordon, S., Hill, A.V., Vannberg, F.O., 2013. Genetic variants of MARCO are associated with susceptibility to pulmonary tuberculosis in a Gambian population. BMC Med. Genet. 14, 47.

Caballero, M.T., Serra, M.E., Acosta, P.L., Marzec, J., Gibbons, L., Salim, M., Rodriguez, A., Reynaldi, A., Garcia, A., Bado, D., et al., 2015. TLR4 genotype and environmental LPS mediate RSV bronchiolitis through Th2 polarization. J. Clin. Invest. 125, 571–582.

Cabello, N., Mishra, V., Sinha, U., DiAngelo, S.L., Chroneos, Z.C., Ekpa, N.A., Cooper, T.K., Caruso, C.R., Silveyra, P., 2015. Sex differences in the expression of lung inflammatory mediators in response to ozone. Am. J. Phys. Lung Cell. Mol. Phys. 309, L1150–L1163.

Carey, M.A., Card, J.W., Voltz, J.W., Germolec, D.R., Korach, K.S., Zeldin, D.C., 2007. The impact of sex and sex hormones on lung physiology and disease: lessons from animal studies. Am. J. Phys. Lung Cell. Mol. Phys. 293, L272–L278.

Cho, H.Y., Zhang, L.Y., Kleeberger, S.R., 2001. Ozone-induced lung inflammation and hyperreactivity are mediated via tumor necrosis factor-alpha receptors. Am. J. Phys. Lung Cell. Mol. Phys. 280, L537–L546.

Cho, H.Y., Morgan, D.L., Bauer, A.K., Kleeberger, S.R., 2007. Signal transduction pathways of tumor necrosis factor–mediated lung injury induced by ozone in mice. Am. J. Respir. Crit. Care Med. 175, 829–839.

Cho, H.Y., Imani, F., Miller-DeGraff, L., Walters, D., Melendi, G.A., Yamamoto, M., Polack, F.P., Kleeberger, S.R., 2009. Antiviral activity of Nrf2 in a murine model of respiratory syncytial virus disease. Am. J. Respir. Crit. Care Med. 179, 138–150.

Cho, H.Y., van Houten, B., Wang, X., Miller-DeGraff, L., Fostel, J., Gladwell, W., Perrow, L., Panduri, V., Kobzik, L., Yamamoto, M., et al., 2012. Targeted deletion of nrf2 impairs lung development and oxidant injury in neonatal mice. Antioxid. Redox Signal. 17, 1066–1082.

Cho, H.Y., Jedlicka, A.E., Gladwell, W., Marzec, J., McCaw, Z.R., Bienstock, R.J., Kleeberger, S.R., 2015. Association of Nrf2 polymorphism haplotypes with acute lung injury phenotypes in inbred strains of mice. Antioxid. Redox Signal. 22, 325–338.

Ciencewicki, J.M., Wang, X., Marzec, J., Serra, M.E., Bell, D.A., Polack, F.P., Kleeberger, S.R., 2014. A genetic model of differential susceptibility to human respiratory syncytial virus (RSV) infection. FASEB J. 28, 1947–1956.

Dahl, M., Bauer, A.K., Arredouani, M., Soininen, R., Tryggvason, K., Kleeberger, S.R., Kobzik, L., 2007. Protection against inhaled oxidants through scavenging of oxidized lipids by macrophage receptors MARCO and SR-AI/II. J. Clin. Invest. 117, 757–764.

Dakhama, A., Lee, Y.M., Gelfand, E.W., 2005. Virus-induced airway dysfunction: pathogenesis and biomechanisms. Pediatr. Infect. Dis. J. 24, S159–S169 (discussion S166–157).

Daley, D., Park, J.E., He, J.Q., Yan, J., Akhabir, L., Stefanowicz, D., Becker, A.B., Chan-Yeung, M., Bosse, Y., Kozyrskyj, A.L., et al., 2012. Associations and interactions of genetic polymorphisms in innate immunity genes with early viral infections and susceptibility to asthma and asthma-related phenotypes. J. Allergy Clin. Immunol. 130, 1284–1293.

Edwards, M.R., Bartlett, N.W., Hussell, T., Openshaw, P., Johnston, S.L., 2012. The microbiology of asthma. Nat. Rev. Microbiol. 10, 459–471.

Epstein, M.P., Allen, A.S., Satten, G.A., 2007. A simple and improved correction for population stratification in case-control studies. Am. J. Hum. Genet. 80, 921–930.

Falsey, A.R., Hennessey, P.A., Formica, M.A., Cox, C., Walsh, E.E., 2005. Respiratory syncytial virus infection in elderly and high-risk adults. N. Engl. J. Med. 352, 1749–1759.

Feldman, A.S., He, Y., Moore, M.L., Hershenson, M.B., Hartert, T.V., 2015. Toward primary prevention of asthma. Reviewing the evidence for early-life respiratory viral infections as modifiable risk factors to prevent childhood asthma. Am. J. Respir. Crit. Care Med. 191, 34–44.

Fjaerli, H.O., Bukholm, G., Krog, A., Skjaeret, C., Holden, M., Nakstad, B., 2006. Whole blood gene expression in infants with respiratory syncytial virus bronchiolitis. BMC Infect. Dis. 6, 175.

Gatti, D.M., Shabalin, A.A., Lam, T.C., Wright, F.A., Rusyn, I., Nobel, A.B., 2009. FastMap: fast eQTL mapping in homozygous populations. Bioinformatics 25, 482–489.

Gelfand, E.W., 2012. Development of asthma is determined by the age-dependent host response to respiratory virus infection: therapeutic implications. Curr. Opin. Immunol. 24, 713–719.

Getts, D.R., Terry, R.L., Getts, M.T., Deffrasnes, C., Muller, M., van Vreden, C., Ashhurst, T.M., Chami, B., McCarthy, D., Wu, H., et al., 2014. Therapeutic inflammatory monocyte modulation using immune-modifying microparticles. Sci. Transl. Med. 6, 219ra217.

Ghosh, S., Gregory, D., Smith, A., Kobzik, L., 2011. MARCO regulates early inflammatory responses against influenza: a useful macrophage function with adverse outcome. Am. J. Respir. Cell Mol. Biol. 45, 1036–1044.

Harkema, J.R., Plopper, C.G., Hyde, D.M., St George, J.A., 1987. Regional differences in quantities of histochemically detectable mucosubstances in nasal, paranasal, and nasopharyngeal epithelium of the bonnet monkey. J. Histochem. Cytochem. 35, 279–286.

Harvey, C.J., Thimmulappa, R.K., Sethi, S., Kong, X., Yarmus, L., Brown, R.H., Feller-Kopman, D., Wise, R., Biswal, S., 2011. Targeting Nrf2 signaling improves bacterial clearance by alveolar macrophages in patients with COPD and in a mouse model. Sci. Transl. Med. 3, 78ra32.

Issuree, P.D., Maretzky, T., McIlwain, D.R., Monette, S., Qing, X., Lang, P.A., Swendeman, S.L., Park-Min, K.H., Binder, N., Kalliolias, G.D., et al., 2013. iRHOM2 is a critical pathogenic mediator of inflammatory arthritis. J. Clin. Invest. 123, 928–932.

Kok, W.L., Denney, L., Benam, K., Cole, S., Clelland, C., McMichael, A.J., Ho, L.P., 2012. Pivotal Advance: invariant NKT cells reduce accumulation of inflammatory monocytes in the lungs and decrease immune-pathology during severe influenza A virus infection. J. Leukoc. Biol. 91, 357–368.

Larcombe, A.N., Foong, R.E., Bozanich, E.M., Berry, L.J., Garratt, L.W., Gualano, R.C., Jones, J.E., Dousha, L.F., Zosky, G.R., Sly, P.D., 2011. Sexual dimorphism in lung function responses to acute influenza A infection. Influenza Other Respir. Viruses 5, 334–342.

Leontyev, D., Katsman, Y., Branch, D.R., 2012. Mouse background and IVIG dosage are critical in establishing the role of inhibitory Fcgamma receptor for the amelioration of experimental ITP. Blood 119, 5261–5264.

Li, M., Wetzel-Strong, S.E., Hua, X., Tilley, S.L., Oswald, E., Krummel, M.F., Caron, K.M., 2014. Deficiency of RAMP1 attenuates antigen-induced airway hyperresponsiveness in mice. PLoS One 9, e102356.

Lightfoot, J.T., Turner, M.J., Daves, M., Vordermark, A., Kleeberger, S.R., 2004. Genetic influence on daily wheel running activity level. Physiol. Genomics 19, 270–276.

Lozano, R., Naghavi, M., Foreman, K., Lim, S., Shibuya, K., Aboyans, V., Abraham, J., Adair, T., Aggarwal, R., Ahn, S.Y., et al., 2012. Global and regional mortality from 235 causes of death for 20 age groups in 1990 and 2010: a systematic analysis for the Global Burden of Disease Study 2010. Lancet 380, 2095–2128.

Lukacs, N.W., Moore, M.L., Rudd, B.D., Berlin, A.A., Collins, R.D., Olson, S.J., Ho, S.B., Peebles Jr., R.S., 2006. Differential immune responses and pulmonary pathophysiology are induced by two different strains of respiratory syncytial virus. Am. J. Pathol. 169, 977–986.

Marzec, J.M., Christie, J.D., Reddy, S.P., Jedlicka, A.E., Vuong, H., Lanken, P.N., Aplenc, R., Yamamoto, T., Yamamoto, M., Cho, H.Y., et al., 2007. Functional polymorphisms in the transcription factor NRF2 in humans increase the risk of acute lung injury. FASEB J. 21, 2237–2246.

McClurg, P., Pletcher, M.T., Wiltshire, T., Su, A.I., 2006. Comparative analysis of haplotype association mapping algorithms. BMC Bioinformatics 7, 61.

Miyairi, I., DeVincenzo, J.P., 2008. Human genetic factors and respiratory syncytial virus disease severity. Clin. Microbiol. Rev. 21, 686–703.

Mukherjee, S., Lukacs, N.W., 2013. Innate immune responses to respiratory syncytial virus infection. Curr. Top. Microbiol. Immunol. 372, 139–154.

Nichols, J.L., Gladwell, W., Verhein, K.C., Cho, H.Y., Wess, J., Suzuki, O., Wiltshire, T., Kleeberger, S.R., 2014. Genome-wide association mapping of acute lung injury in neonatal inbred mice. FASEB J. 28, 2538–2550.

Obata, K., Kojima, T., Masaki, T., Okabayashi, T., Yokota, S., Hirakawa, S., Nomura, K., Takasawa, A., Murata, M., Tanaka, S., et al., 2013. Curcumin prevents replication of respiratory syncytial virus and the epithelial responses to it in human nasal epithelial cells. PLoS One 8, e70225.

Pletcher, M.T., McClurg, P., Batalov, S., Su, A.I., Barnes, S.W., Lagler, E., Korstanje, R., Wang, X., Nusskern, D., Bogue, M.A., et al., 2004. Use of a dense single nucleotide polymorphism map for in silico mapping in the mouse. PLoS Biol. 2, e393.

Prince, G.A., Horswood, R.L., Berndt, J., Suffin, S.C., Chanock, R.M., 1979. Respiratory syncytial virus infection in inbred mice. Infect. Immun. 26, 764–766.

Rogers, N.J., Lees, M.J., Gabriel, L., Maniati, E., Rose, S.J., Potter, P.K., Morley, B.J., 2009. A defect in Marco expression contributes to systemic lupus erythematosus development via failure to clear apoptotic cells. J. Immunol. 182, 1982–1990.

Saltini, C., Hance, A.J., Ferrans, V.J., Basset, F., Bitterman, P.B., Crystal, R.G., 1984. Accurate quantification of cells recovered by bronchoalveolar lavage. Am. Rev. Respir. Dis. 130, 650–658.

Stark, J.M., McDowell, S.A., Koenigsknecht, V., Prows, D.R., Leikauf, J.E., Le Vine, A.M., Leikauf, G.D., 2002. Genetic susceptibility to respiratory syncytial virus infection in inbred mice. J. Med. Virol. 67, 92–100.

Stark, J.M., Barmada, M.M., Winterberg, A.V., Majumber, N., Gibbons Jr., W.J., Stark, M.A., Sartor, M.A., Medvedovic, M., Kolls, J., Bein, K., et al., 2010. Genomewide association analysis of respiratory syncytial virus infection in mice. J. Virol. 84, 2257–2269.

Stoppelenburg, A.J., Salimi, V., Hennus, M., Plantinga, M., Huis in 't Veld, R., Walk, J., Meerding, J., Coenjaerts, F., Bont, L., Boes, M., 2013. Local IL-17A potentiates early neutrophil recruitment to the respiratory tract during severe RSV infection. PLoS One 8, e78461.

Thakur, S.A., Hamilton Jr., R.F., Holian, A., 2008. Role of scavenger receptor a family in lung inflammation from exposure to environmental particles. J. Immunotoxicol. 5, 151–157.

Thakur, S.A., Beamer, C.A., Migliaccio, C.T., Holian, A., 2009. Critical role of MARCO in crystalline silica-induced pulmonary inflammation. Toxicol. Sci. 108, 462–471.

Thomsen, M., Nordestgaard, B.G., Kobzik, L., Dahl, M., 2013. Genetic variation in the scavenger receptor MARCO and its association with chronic obstructive pulmonary disease and lung infection in 10,604 individuals. Respiration 85, 144–153.

Tsaih, S.W., Korstanje, R., 2009. Haplotype association mapping in mice. Methods Mol. Biol. 573, 213–222.

Varga, S.M., Braciale, T.J., 2013. The adaptive immune response to respiratory syncytial virus. Curr. Top. Microbiol. Immunol. 372, 155–171.

Yoo, J.K., Kim, T.S., Hufford, M.M., Braciale, T.J., 2013. Viral infection of the lung: host response and sequelae. J. Allergy Clin. Immunol. 132, 1263–1276 (quiz 1277).